

# The accretion history of the Universe with the SKA

Matt J. Jarvis\* and Steve Rawlings†

Astrophysics, Department of Physics, Keble Road, Oxford, OX1 3RH, UK

In this paper we investigate how the Square Kilometre Array (SKA) can aid in determining the evolutionary history of active galactic nuclei (AGN) from redshifts  $z = 0 \rightarrow 6$ . Given the vast collecting area of the SKA, it will be sensitive to both ‘radio-loud’ AGN and the much more abundant ‘radio-quiet’ AGN, namely the radio-quiet quasars and their ‘Type-II’ counterparts, out to the highest redshifts. Not only will the SKA detect these sources but it will also often be able to measure their redshifts via the Hydrogen 21 cm line in emission and/or absorption. We construct a complete radio luminosity function (RLF) for AGN, combining the most recent determinations for powerful radio sources with an estimate of the RLF for radio-quiet objects using the hard X-ray luminosity function of Ueda et al. (2003), including both Type-I and Type-II AGN. We use this complete RLF to determine the optimal design of the SKA for investigating the accretion history of the Universe for which it is likely to be a uniquely powerful instrument.

## 1. INTRODUCTION

Radio astronomy has played an important rôle in the hunt for high-redshift active galactic nuclei (AGN), with very-high-redshift objects being pinpointed by radio pre-selection: at low radio frequency finding ‘steep-spectrum’ radio galaxies (Rawlings et al., 1996; van Breugel et al., 1999) out to redshift  $z \sim 5$ ; and at high frequency finding similarly distant ‘flat-spectrum’ (or ‘Giga-Hertz-Spectrum’ GPS) quasars (e.g. Hook et al., 2002). The obvious benefits of radio pre-selection remain, e.g. the fact that obscuration by dust and neutral Hydrogen is unimportant, contrasting dramatically with the case for optical and X-ray surveys.

The reason why radio surveys led the way for so long is because a radio-loud source is essentially detectable out to the very highest redshifts with only a moderate exposure time, e.g. the highest redshift radio galaxy discovered to date was selected from the Westerbork Northern Sky Survey (WENSS<sup>3</sup>; Rengelink et al. (1997)) and has a flux density of  $S_{365\text{MHz}} \sim 0.6$  Jy. Another advantage of radio surveys is that, particularly at the lower frequencies, the sky coverage per pointing can be

huge, e.g. for the new 74 MHz extension at the VLA the field-of-view (FOV) is  $\sim 40$  deg<sup>2</sup>, much larger than any FOV on an optical or X-ray telescope.

However, genuinely radio-loud sources are rare, probably  $\sim 10 - 100$  times less abundant than their radio-quiet counterparts (Goldschmidt et al., 1999), whereas the optical (Fan et al., 2001a,b, 2003), and (with the advent of XMM-Newton and CHANDRA) the X-ray surveys are now taking the lead in surveying AGN in the high-redshift Universe (e.g. Barger et al., 2003a,b). The results of these surveys are providing us with a much better understanding of both the unobscured and obscured AGN populations, in the case of the Sloan Digital Sky Survey (SDSS; Schneider et al., 2003) *and*, on the traditional ground of the radio telescope, the X-ray satellites are giving a much more transparent view of the more obscured population (Norman et al., 2002). Unfortunately, there are still many unresolved issues, most obviously highlighted by the fact that about 50% of the hard X-ray background is still unresolved into discrete AGN, the consensus being that the current generation of X-ray telescopes, operating at  $0.5 \rightarrow 12$  keV, are missing the highly obscured sources, with Hydrogen column densities  $N_{\text{H}} > 10^{28} \text{ m}^{-2}$  (Wilman, Fabian, & Nulsen,

\*mjj@astro.ox.ac.uk

†s.rawlings1@physics.ox.ac.uk

<sup>3</sup><http://www.strw.leidenuniv.nl/wenss>

2000; Ueda et al., 2003; Gandhi et al., 2004).

The SDSS and ultra-deep X-rays fields are paving the way (e.g. Brandt et al., 2001; Alexander et al., 2003b) but the quest to determine the nature and, possibly more importantly, the evolution in the obscured population is liable to switch back to the realm of radio astronomy with the commissioning of the next generation of radio telescopes, most notably the Low-Frequency Array (LOFAR<sup>4</sup>) and the Square Kilometre Array (SKA<sup>5</sup>).

The LOFAR is currently set to operate at the very-low-frequency ( $< 250$  MHz) end of the radio spectrum, where the Universe has, to date, not been deeply explored. This will allow an unprecedented view of the highest redshift AGN, where the intrinsic spectral shape of a radio-loud AGN means that the most sensitivity is gained at the lowest frequencies. Coupled with the fact that the 21 cm Hydrogen (HI) line is redshifted to below 200 MHz at  $z > 6$ , where the epoch of reionization is coming to an end (Becker et al., 2001), this means that the LOFAR will be able to probe the neutral Hydrogen within the epoch of reionization, as opposed to the optical waveband where the Gunn-Peterson trough due to neutral Hydrogen extinguishes Lyman- $\alpha$  photons (Gunn & Peterson, 1965). However the LOFAR, although important for many studies of the AGN population, will not be able to secure redshifts for the vast majority of the radio sources it finds, and as such optical and near-infrared spectroscopy will always be needed. Moreover, due to the large source density at the faintest flux-density limits, selection criteria based on the radio spectral properties will still be required in order to disentangle the highest redshift sources from the more prominent low-redshift population (e.g. Röttgering et al., 1994; Chambers et al., 1996; Röttgering et al., 1997; Blundell et al., 1998; Jarvis et al., 2001a,b; De Breuck et al., 2001)

A more promising telescope in terms of constraining the evolution and properties of the AGN population is the SKA. With the proposed sensi-

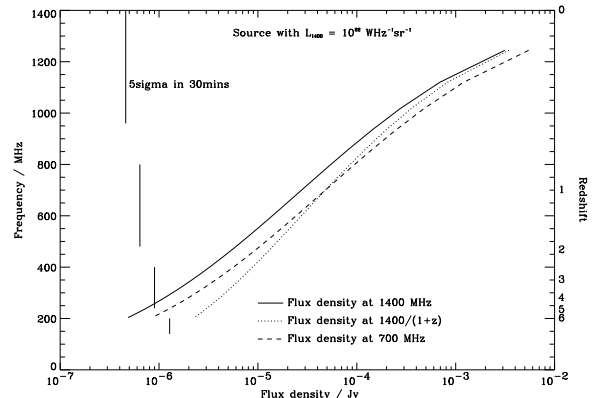


Figure 1. The flux density of a ‘radio-quiet’ AGN with  $L_{1.4\text{GHz}} = 10^{22} \text{ W Hz}^{-1} \text{ sr}^{-1}$  and  $\alpha = 0.8$ , as a function of redshift and observing frequency. The solid line is the flux-density measured at the observed frequency of 1400 MHz; the dashed line is the flux density measured at 700 MHz and the dotted line is the flux density measured at the frequency of redshifted HI.

tivities, the SKA will be able to detect all the radio-loud and radio-quiet<sup>6</sup> AGN up to and including the epoch of reionization at  $z > 6$  in a  $\sim 30$ -minute integration (Fig. 1). The capabilities of the SKA for probing AGN within the Epoch of Reionization are considered in Carilli et al. (this volume). The SKA also has the capability to measure the redshifts of many of the sources it detects via the HI line in emission or absorption. A three-dimensional picture of the *whole* of the AGN population will become apparent immediately.

In this paper we investigate what the SKA will be able to contribute to studies of the whole of the AGN population, both ‘radio loud’ and ‘radio quiet’ (see also Jackson, this volume; Falcke, Körtling & Nagar, this volume). In Section 2 we

<sup>6</sup>A characteristic value of  $L_{1.4\text{GHz}} = 10^{22} \text{ W Hz}^{-1} \text{ sr}^{-1}$  is chosen for ‘radio-quiet’ AGN above which (roughly speaking) weak-AGN-dominated radio emitters dominate, and below which starburst-dominated radio emitters dominate.

<sup>4</sup><http://www.lofar.org>

<sup>5</sup><http://www.skatelescope.org>

describe the form of the radio luminosity function (RLF) for the powerful radio-loud AGN. In Section 3 we show how to translate the hard-X-ray luminosity function to that of an RLF for the radio-quiet AGN population. Adding these together yields a *complete* radio luminosity function for AGN, described in Section 4. In section 5 we estimate what the SKA will see in terms of AGN and in Section 6 we investigate the optimum design for the SKA in terms of constraining the evolution of the entire AGN population. In Section 7 we outline some of the science that the SKA is likely to deliver.

We adopt a  $\Lambda$ CDM cosmology with the following parameters:  $h = H_0/(100 \text{ km s}^{-1} \text{ Mpc}^{-1}) = 0.7$ ;  $\Omega_m = 0.3$ ;  $\Omega_\Lambda = 0.7$ , throughout. We define radio spectral index as  $S_\nu \propto \nu^{-\alpha}$ , where  $S_\nu$  is the radio flux density at frequency  $\nu$ .

## 2. The radio-loud luminosity function

The radio-loud population can be split into two types of source, with a division (roughly speaking) at a critical radio luminosity in radio structure (Fanaroff & Riley, 1974), narrow-emission-line strength (Hine & Longair, 1979) and quasar fraction (Willott et al., 2000). Below a radio luminosity  $L_{1.4\text{GHz}} \sim 10^{25} \text{ W Hz}^{-1} \text{ sr}^{-1}$ , objects are typically FRI radio galaxies with weak or absent emission lines. Above the break in the RLF (at  $L_{1.4\text{GHz}} \sim 10^{26} \text{ W Hz}^{-1} \text{ sr}^{-1}$ ), objects are a roughly equal mix of FRII radio galaxies and FRII radio quasars, typically with strong emission lines, indicating buried quasar nuclei even in the cases where no direct quasar emission is evident. The transition region between these two sub-populations lies just below the break in the RLF. The vast majority of work in constraining the evolution in the luminosity function of the powerful radio sources has concentrated on the ‘FRII sub-population’, due mainly to the fact that the low radio luminosities of FRI sources makes them hard to detect out to the highest redshifts.

### 2.1. The high-luminosity RLF: FRIIs

The form of the RLF for the FRII sub-population has been constrained to a certain de-

gree by the work of Dunlop & Peacock (1990), and more recently Willott et al. (2001). Here we use one of the parameterized models of Willott et al. (model C) which describes the high-luminosity population by a ‘reversed Schechter function’ with an evolutionary term fitted with two one-sided Gaussian functions, forced to match at a peak redshift of  $z = 1.9$ . The form of this RLF means that the increase in source density towards this redshift is much steeper than the higher redshift decline. However, the data used by Willott et al. (2001) to model the RLF has a dearth of sources at high redshift due to a high flux-density limit for the large area samples (e.g. 3CRR; Laing, Riley, & Longair, 1983) and a lack of sky area for the faint flux-density samples (6CE and 7CRS; Eales et al., 1997; Rawlings, Eales, & Lacy, 2001; Willott et al., 2002, 2003). Thus, the high-redshift evolution is not yet well constrained.

The form of the decline in the comoving space density at high redshift has come under close scrutiny from a number of groups, some of which suggest quite a steep decline at  $z > 3$  (Shaver et al., 1996), and some of which suggest a more moderate decline (e.g. Dunlop & Peacock, 1990). However Jarvis & Rawlings (2000) and Jarvis et al. (2001c) highlighted how uncertain the form of this decline is for both flat-spectrum radio-loud quasars (which, crudely speaking, should reflect the overall evolution as it picks out favourably oriented sources from the underlying population) and also low-frequency-selected radio galaxies, due predominantly to difficulties in modelling the  $k$ -corrections, and the lack of available volume (and hence small numbers of sources) at high redshift for a given flux-density-limited sample. This uncertainty is also mirrored by the X-ray luminosity function (e.g. Miyaji, Hasinger, & Schmidt, 2000; Ueda et al., 2003, see also Section 3). Our adopted model lies between the extremes of a sharp cut off and an RLF which stays constant with redshift at  $z > 2$ . Such an evolution is consistent with the predictions of simple Press-Schechter-based theoretical models (Rawlings & Jarvis, 2004).

## 2.2. The moderate-luminosity RLF: FRIs

Unfortunately, the RLF for the lower-luminosity radio-loud AGN, predominantly (but not exclusively) comprised of FRI radio sources, hereafter the ‘FRI sub-population’, is poorly constrained. Several groups have reached different conclusions concerning their evolutionary behaviour (e.g. Jackson & Wall, 1999; Snellen & Best, 2001; Clewley & Jarvis, 2004). Here we adapt the results of Clewley & Jarvis (2004), who used the largest dataset of  $\sim 1000$  sources, with a radio flux-density limit of  $S_{325\text{MHz}} = 40$  mJy, with photometric redshifts determined by five-colour photometry of the SDSS, to show that radio sources with  $10^{23} \leq (L_{325\text{MHz}} / \text{W Hz}^{-1} \text{ sr}^{-1}) \leq 10^{25}$  are consistent with having a constant comoving density, at least in the redshift range  $z = 0 \rightarrow 0.5$ . We also note that the results of their analysis are consistent with that of Waddington et al. (2001), who constrained the form of the evolution using a much fainter flux-density limited survey (LBDS; Waddington et al., 2000) but with a higher fraction of redshift incompleteness. We allow this sub-population to have a comoving space density which evolves very mildly with redshift as  $\Phi \propto (1+z)^{1.2}$ , normalised to the comoving space density of this sub-population from the model of Willott et al. at  $z = 0.5$ , i.e. where redshift data are able to directly constrain the space density.

## 3. The low-luminosity RLF: radio-quiet

As stated in Section 1 the SKA will have the sensitivity to trace radio-quiet quasars and radio-quiet type-II AGN out to the highest redshifts. Therefore, we have attempted to parameterize the form of the radio-quiet RLF and its evolution with redshift. The work of Kukula et al. (1998) suggested that the radio emission from radio-quiet quasars is typically compact and is probably directly associated with the central engine. They also showed that radio-quiet quasars have spectral indices consistent with their more radio-loud counterparts, i.e.  $\alpha \sim 0.7$ .

We also know that the X-ray luminosity of an AGN is a good tracer of the accretion rate onto the SMBH. Thus, there should be a link between

the X-ray luminosity and the radio luminosity if both are regulated by the accretion process. Indeed, Brinkmann et al. (2000) show that this link does exist. They compiled a sample of X-ray selected AGN from the ROSAT All-Sky Survey (Voges et al., 1999) and cross-correlated this sample with the 1.4 GHz FIRST survey (White et al., 1997). They find a relatively tight linear correlation between the logarithm of radio luminosity at 1.4 GHz and the X-ray luminosity in the soft X-ray band at 0.5-2 keV band. The form of this correlation is

$$\log(L_X) = -4.57 + 1.012 \log(L_{1.4\text{GHz}}), \quad (1)$$

i.e. roughly a proportionality. With this in mind, it is possible to use a complete description of the radio-quiet quasar population in the X-ray band to make a *crude estimate* of the RLF of radio-quiet objects at 1.4 GHz.

With the advent of XMM-Newton and Chandra, and the deep fields surveyed with these satellites, a hard X-ray luminosity function (XLF) has been determined by Ueda et al. (2003), building on the work of Miyaji, Hasinger, & Schmidt (2000) in the softer X-ray bands. They find that the best parameterisation of the XLF is one of luminosity-dependent density evolution, i.e. one in which the cosmic evolution in the space density of the sources depends on the intrinsic luminosity of the source. They conclude that the comoving space density of the more X-ray-luminous AGN peaked at an earlier epoch than those at lower X-ray luminosities. The evidence for this type of evolution is reinforced by other studies (e.g. Steffen et al., 2003). They also find that the higher luminosity sources have less intrinsic absorption, consistent with a ‘receding-torus-like’ model (e.g. Lawrence, 1991) which has been suggested as a necessary physical ingredient to explain the properties of radio-selected samples (e.g. Simpson, 1998; Willott et al., 2000; Grimes, Rawlings, & Willott, 2004).

With this parameterization, we predict how many X-ray sources there will be of a given luminosity in the (rest frame) 2  $\rightarrow$  10 keV energy range, at a given redshift. We use the rest-frame ratio of the average number of photons in

this band to that of the monochromatic luminosity at 1 keV for an unobscured source, noting that the quasars were predominantly unobscured in the study of Brinkmann et al. (2000). We then convert this soft-X-ray luminosity to the 1.4 GHz radio luminosity using Equation 1. In addition, we need to take some account of a population of highly-obscured (Compton thick) AGN, which, whilst essentially absent from the existing ‘hard’ (2-10 keV) surveys, would be revealed by still harder X-ray surveys (Wilman & Fabian, 1999) with the next generation of X-ray satellites (e.g. XEUS<sup>7</sup> and Constellation-X<sup>8</sup>) or radio surveys. To do this we multiply the comoving space density derived from the XLF by a conservative factor of 1.5 to account for the X-ray obscured sources, which brings the integrated luminosity closer to that expected from the hard-X-ray background.

#### 4. The complete RLF and constraints from the source counts

In Figure 2 we show the complete RLF, incorporating the radio-loud sources (consisting of the two FRI and FRII sub-populations following Willott et al. (2001)) and the radio-quiet quasars. This is the RLF we use to predict what the SKA will see in terms of AGN for various SKA designs. With this parameterisation of the RLF we can make a consistency check with the radio source counts at 1.4 GHz. In Figure 3 we show the radio source counts at 1.4 GHz down to a flux-density limit of  $S_{1.4\text{GHz}} \sim 1 \mu\text{Jy}$ , along with the source counts derived from our RLF.

One can see immediately that the RLF traces the source counts reasonably well at the high-flux-density regime, as it should do, as this is where direct constraints from data exist. The small deviations are artefacts of the ‘two-sub-population’ method which would be removed by using smoother functional forms (such as the ‘free-form’ fits of Dunlop & Peacock (1990) or the generalized luminosity functions of Grimes, Rawlings, & Willott (2004)). At lower radio flux densities the moderate-luminosity ‘FRI’

AGN begin to dominate the source counts, but at lower flux densities still ( $S_{1.4\text{GHz}} \sim 5 \times 10^{-4} \text{ Jy}$ ) the radio-quiet population can start to contribute significantly to the source counts. The upturn in the source counts around this flux density is often attributed solely to a low-redshift, star-forming population. However as can be seen from Fig. 3 the radio-quiet population, comprising radio-quiet quasars and their ‘Type-II’ counterparts (including Compton-thick sources) may contribute significantly to this upturn (see also Baugh et al., this volume). Of course, starburst-driven radio emission may make an important contribution to the radio flux densities of at least some radio quiet quasars (e.g. Sopp & Alexander, 1992; Prouten et al., 2004), and ‘starburst’ galaxies seem commonly to harbour X-ray (AGN) nuclei (e.g. Alexander et al., 2003a), so the distinction between these two populations is not particularly clear. The starburst population is considered elsewhere (van der Hulst et al., this volume), and it is clear from Fig. 3 that as we approach the depths of even shallow SKA surveys (surveys limited at  $\sim \mu\text{Jy}$  levels), a small fraction of the objects are likely to have their radio emission powered by any sort of AGN activity.

Our description of the radio luminosity function, although very crude, allows us to at least estimate the contributions from the various populations of radio AGN. As such we can distinguish between those with massive black holes but low accretion rates (FRIs) and those with massive black holes and high accretion rates (the radio-quiet quasars). However, it is worth noting that Blundell & Rawlings (2001) have shown that both classes can produce similar radio luminosities and radio structures. Ideally, a complete model for the evolution of all AGN in radio wavebands would allow for more physically driven processes, with a more continuous level of accretion between the various classes (or equivalently less of a dichotomy between ‘radio-loud’ and ‘radio-quiet’ sources).

Also, we have not attempted to add prescriptions for favourably-oriented, and hence Doppler-boosted (flat-spectrum) sources and young (GPS) sources as we will detect every AGN with the SKA and these sources do not make up the bulk

<sup>7</sup><http://www.rssd.esa.int/XEUS>

<sup>8</sup><http://constellation.gsfc.nasa.gov>

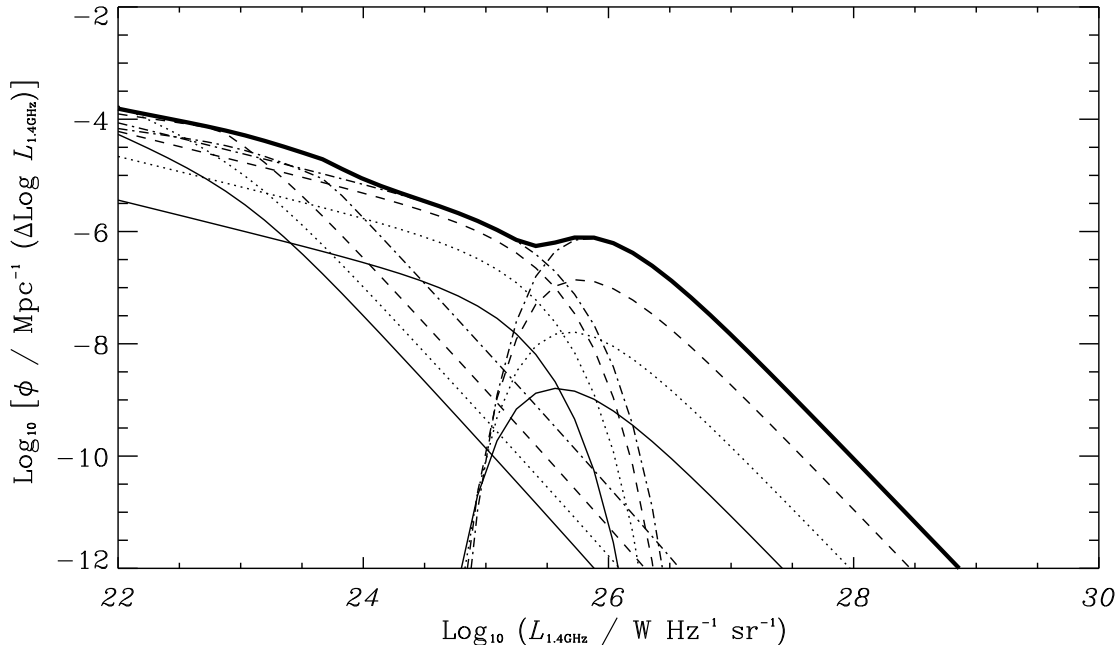


Figure 2. The 1.4 GHz radio luminosity function for all AGN at four different redshifts. The contributions from the radio-quiet quasar population can be seen to be significant between  $10^{22} < (L_{1.4}/W \text{ Hz}^{-1} \text{ sr}^{-1}) < 10^{24}$ , whereas the bulk of the radio luminosity density is provided by the FRI-type sources at  $L_{1.4} \sim 10^{25} \text{ W Hz}^{-1} \text{ sr}^{-1}$ . Finally, at  $L_{1.4} > 10^{26} \text{ W Hz}^{-1} \text{ sr}^{-1}$  all of the luminosity density is provided by the powerful FRII-type sources. The thin solid line is the RLF for each sub-population at  $z = 0$ , the dotted line is at  $z = 0.5$ , the dashed line is the RLF at  $z = 1$  and the dot-dashed line is the RLF at  $z = 2$ . To clarify the overall form, the thick solid line represents the composite RLF, comprised of the FRII, FRI and radio-quiet populations described in Section 2 at  $z = 2$ .

of the population when probing such low flux-density limits.

Again, more realistic models could allow for factors such as the time evolution of radio luminosity (although we caution that such models bring in lots of uncertain physical details such as evolutions in environment, and the behaviour of jet power as a function of time).

However, regardless of all such details, with a crude composite RLF in place we are able to make a crude prediction of the number of each type of AGN the SKA will be able to detect as a function of flux density and area.

## 5. What will the SKA see?

### 5.1. The number of AGN detected by the SKA in 1 year

Using the composite RLF discussed in Section 2 we are able to estimate the number of sources that the SKA will be able to detect as a function of both redshift and flux-density limit. In Fig. 4 we plot the predicted  $dN/dz$  distribution for each sub-population in an all-hemisphere SKA survey which would reach a limiting ( $4\sigma$ ) flux-density limit of  $S_{200\text{MHz}} = 100 \text{ nJy}$  in one year of

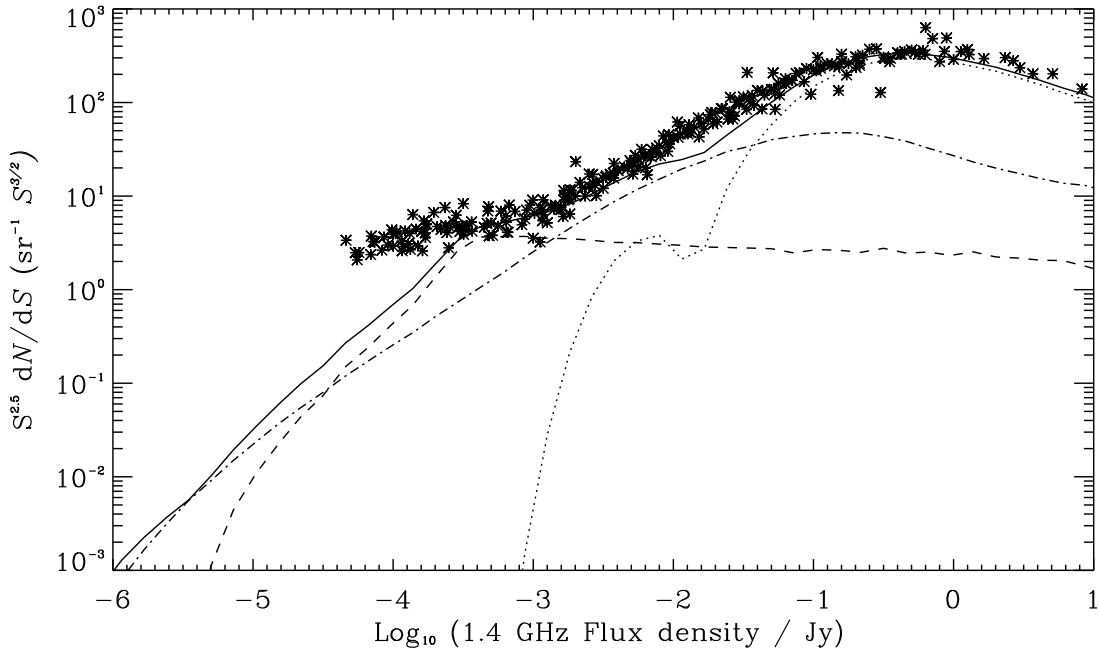


Figure 3. The 1.4 GHz differential source counts (relative to counts in a Euclidean Universe) of a combination of surveys (see Seymour, McHardy & Gunn, 2004, for a description of the data points). The lines represent the model source counts from our three components of the radio luminosity function. The dotted line represents the powerful FRII sources, the dot-dashed line is for the moderate luminosity, typically FRI sources, and the dashed line represents the source counts for radio-quiet quasars. The solid line is the total source counts from these models.

dedicated observations with the SKA<sup>9</sup>.

One can see that the SKA will be able to detect every bona fide AGN in the Universe up to  $z \sim 6$ . It is worth noting that there is a large overlap between what we have called FRI-type AGN and the radio-quiet quasars. This is because it is

<sup>9</sup>This assumes a usable field of view at 200 MHz of  $\approx 50 \text{ deg}^2$  (or  $FOV = 1 \text{ deg}^2$  at 1.4 GHz in the diffraction-limited case), so a survey of  $\sim 20,000 \text{ deg}^2$  requires  $\sim 400$  pointings. A one-year survey (at 90 per cent observing efficiency), means  $\approx 20$  hours of exposure per pointing, yielding a survey rms of  $\approx 25 \text{ nJy}$ . In practice, a ‘tiling’ method will be used to ensure complete sky coverage across the entire 0.2  $\rightarrow$  1.4 GHz range (see Rawlings et al., this volume). For an SKA design with a  $\sim 10$ -times-higher  $FOV$ , a  $10\text{-}\sigma$  catalogue to the same limiting flux density could be compiled from a survey taking eight months.

largely a question of semantics as to what kind of source belongs where (e.g. Blundell & Rawlings, 2001).

It is also worth noting that at high redshift ( $z > 3$ ) all three of the sub-populations are largely unconstrained. Therefore, we force both the FRI-type sources and the radio-quiet sources to decline according to the decrease in space density expected under a Press-Schechter based model (see e.g. Rawlings & Jarvis, 2004) above a redshift of  $z \sim 3$ . For the more powerful, FRII-type sources we just use the shallow decline in the space density described by model C in Willott et al. (2001).

Due to these large extrapolations the ratio be-

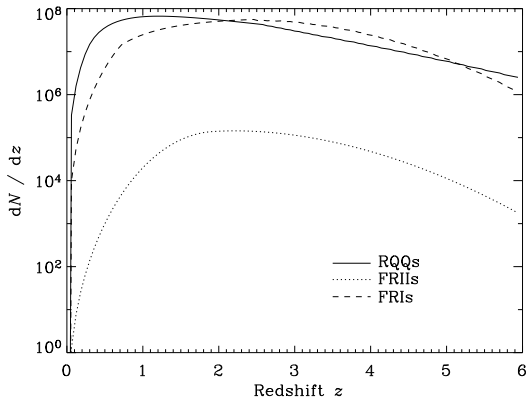


Figure 4. The number of the different sub-classes of sources discussed in Section 4 for a one year SKA survey over one hemisphere ( $\sim 20,000 \text{ deg}^2$ ) complete to  $S_{200\text{MHz}} \sim 100 \text{ nJy}$ . The dotted line represents the powerful FRII-type sources, the dashed line shows the evolution in the FRI-type sources and the solid line denotes the radio-quiet quasars calculated using the XLF of Ueda et al. (2003) and multiplied by a factor of 1.5 (see Section 3).

tween radio-loud sources and radio-quiet sources stays roughly similar to what we observe at  $z < 2$  with today’s telescopes. However, the SKA will actually measure this ratio to great accuracy, and as a consequence may yield strong constraints on AGN driven feedback events (see Section 7 and Rawlings & Jarvis (2004)) and the duty cycle of all types of AGN.

## 5.2. Supermassive black holes and their accretion rate

In this section we estimate what the SKA will be able to see in terms of the accretion rate of black holes with masses in the range  $10^6 M_\odot < M_{\text{bh}} < 10^9 M_\odot$ . To estimate the bolometric luminosity, and thus calculate the fraction of the Eddington luminosity which relates to a given radio luminosity for both the powerful radio-loud sources and the radio-quiet sources we use two

separate methods.

For the radio-loud sources, i.e. those sources above the break in the RLF (see Section 2) we use the relation of Willott et al. (2000) which relates the low-frequency radio luminosity to the total ionizing power of the AGN. This has the form,

$$\log(L_{\text{Bol}}/W) \approx 0.83 \log(L_{151}/W \text{ Hz}^{-1}\text{sr}^{-1}) + 16.9, \quad (2)$$

where  $L_{\text{Bol}}$  is the bolometric luminosity and  $L_{151}$  is the monochromatic luminosity at 151 MHz. We convert the 151 MHz luminosity to 200 MHz using a spectral index of  $\alpha = 0.8$ .

For the case of the radio-quiet quasars (and type-II obscured quasars) we use the ratio of bolometric luminosity to monochromatic luminosity  $L_{2500}$  (at  $2500 \text{ \AA}$ ) from Elvis et al. (1994), along with the newly derived optical–X-ray spectral index  $\alpha_{\text{OX}}$  given in Elvis, Risaliti & Zamorani (2002). We then use the correlation between X-ray luminosity and radio luminosity given in Section 3 to estimate the radio luminosity at 200 MHz (using  $\alpha = 0.7$ ; Kukula et al., 1998).

Fig. 5 shows what the SKA, with a flux-density limit of  $S_{200\text{MHz}} > 100 \text{ nJy}$ , will see in terms of radio-loud quasars (left) and radio-quiet quasars (right) as a fraction of the Eddington luminosity versus redshift for AGN with black-hole masses  $10^6 M_\odot < M_{\text{bh}} < 10^9 M_\odot$ . Given that *powerful* radio sources seem to require a supermassive black hole with mass  $\gtrsim 10^8 M_{\text{bh}}$  (Dunlop et al., 2003; Jarvis & McLure, 2002; McLure et al., 2004; McLure & Jarvis, 2004) then it is obvious from Fig. 5 that the SKA will easily detect all such sources. However, more interestingly the SKA will be able to detect all the radio-quiet quasars with  $M_{\text{bh}} > 10^6 M_\odot$  accreting at  $< 10$  per cent of its Eddington limit up to  $z \sim 6$ . In the case of the powerful quasars being found at high redshift in the SDSS, with black-hole masses  $> 10^9 M_\odot$  (Willott, McLure & Jarvis, 2003), these would be detected up to  $z \sim 6$  if their accretion luminosities were  $\sim 10^{-4} L_{\text{Edd}}$ , i.e. in the realm of what we now consider as dormant black holes.



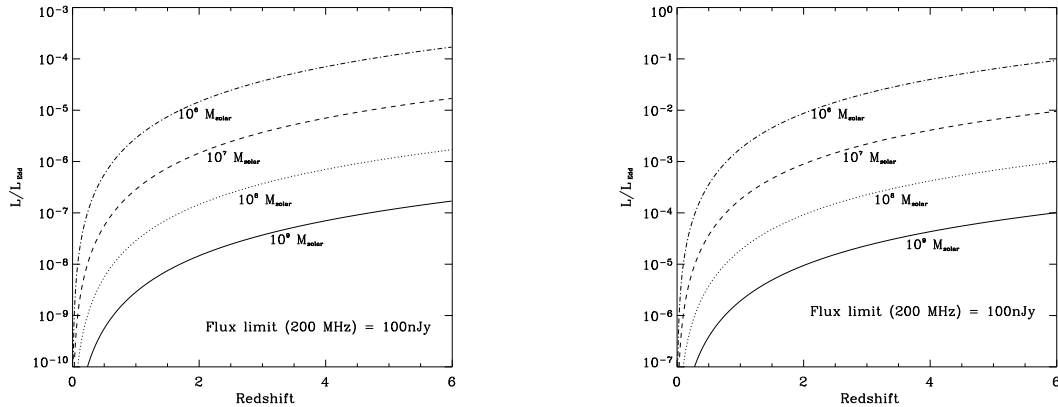


Figure 5. The detectable accretion luminosity  $L/L_{\text{Edd}}$  versus redshift for sources containing black holes of various mass ( $10^6 \rightarrow 10^9 M_{\odot}$ ), at a flux-density limit of  $S_{200\text{MHz}} = 100 \text{ nJy}$  for radio-loud, typically FR II, sources (left) and for radio-quiet sources (right).

## 6. The optimal SKA design

In this section we investigate the most efficient design of the SKA for determining the large scale properties and evolution of the AGN. We only consider those AGN which have an X-ray luminosity  $L_X > 10^{35} \text{ W}$ , i.e. those in the regime where accretion onto a supermassive black hole is the only way of producing such emission and avoiding luminosities where supernovae and X-ray binaries may begin to dominate the population. This means that the SKA will be able to probe the ‘whole AGN population’ up to  $z \sim 6$  by just surveying down to micro-Jansky levels.

One of the crucial points in a survey to map the AGN population at  $0 < z < 6$  with the SKA is that IT MUST be able to observe across the frequency range  $200 < \nu < 1400 \text{ MHz}$ . This is not for the traditional reason of previous low-frequency-based redshift surveys such as 6CE, 6C\* and 7CRS. In these samples the low survey frequency selected sources in an unbiased manner with respect to source orientation, i.e. sources are selected on their optically-thin lobe emission. Low-frequency selection is also used to target the highest redshift radio galaxies (see e.g. Cohen et al., 2004; Jarvis et al., 2004), whereas

traditional high-frequency selection would miss them due to the shape of radio galaxy spectra. The sensitivity of the SKA will mean that this type of ‘low-frequency selection’ is unimportant, as all of the radio sources will easily be detected at 1.4 GHz regardless of the redshift.

However, the crucial advantage that the SKA will have over future X-ray missions in probing the AGN population will be its ability to measure redshifts of all the gas-rich galaxies out to  $z \sim 2$  (Abdalla & Rawlings, 2004) via HI emission. This means that the redshifts of the majority of the source counts at these flux-density levels will already be known. This paves the way for both directly constraining the evolution in the high-redshift population along with their three-dimensional clustering, and to investigate the accretion rate of *all powerful* AGN from  $z = 0 \rightarrow 2$ .

Moreover, powerful AGN, invariably reside in massive galaxies (i.e.  $> L^*$ ; Jarvis et al., 2001b; Willott et al., 2003; McLure et al., 2004) and high-redshift-AGN activity, triggered by mergers, are likely to contain higher gas fractions than at lower redshifts. Evidence for this has been seen in the past few years (e.g. Papadopoulos et al., 2001; Greve, Ivison & Papadopoulos, 2004)

Therefore, the HI emission signature will prob-

ably be detected to higher redshifts than for the less massive galaxies which are detailed in Abdalla & Rawlings (2004). There is also the possibility of utilizing the fact that many AGN, both optically selected and radio selected, exhibit some level of HI absorption in their Lyman- $\alpha$  profiles, (e.g. van Ojik et al., 1997; Jarvis et al., 2003; Wilman et al., 2004). This gas could also be detected against the radio continuum of these distant sources via the HI transition. However, this obviously needs the SKA to operate at lower and lower frequencies depending on the maximum redshift one wishes to probe.

In order to estimate whether the SKA will be able to determine redshifts via HI absorption against radio-loud objects up to  $z \sim 6$  (see also Morganti et al., this volume) we assume a minimum HI column density of  $N_{\text{HI}} = 10^{23} \text{ m}^{-2}$  (or  $N_{\text{HI}} = 10^{19} \text{ cm}^{-2}$ ) and a line width of  $\sim 100 \text{ km s}^{-1}$  which is similar to the absorption systems observed in Lyman- $\alpha$  around high-redshift radio galaxies, (Jarvis et al., 2003; Wilman et al., 2004).

Using equation 1 from Chengalur & Kanekar (2000) with a spin temperature of  $T_{\text{S}} = 100 \text{ K}$  (see e.g. Beswick et al., 2004) and unity covering factor we find a target velocity-integrated optical depth  $\tau dV \approx 0.06 \text{ km s}^{-1}$ . Taking a source at  $z \sim 6$  with a luminosity around the break in the RLF for powerful radio sources, i.e.  $L_{200} \sim 10^{26.5} \text{ W Hz}^{-1} \text{ sr}^{-1}$  gives a flux density at the redshifted frequency of HI of  $S_{200\text{MHz}} \approx 15 \text{ mJy}$ . In the proposed one-year all-sky survey, the expected dip due to HI absorption (at a level  $\sim 6 \times 10^{-4}$  of the continuum) would be detected at  $\approx 10\sigma$  in an optimally-smoothed spectrum.<sup>10</sup>

Obviously, ignoring any cosmic evolution in the HI properties, the situation<sup>11</sup> becomes much better at lower redshift where higher sensitivities are reached for a source of the same luminosity as the one considered at  $z \sim 6$ . Therefore, we envisage that the SKA will be able to detect and measure the redshift of almost every ‘FRII-like’ AGN in the Universe up to at least  $z \sim 6$ , if

these sources lie within a shell of HI gas with column densities  $\sim 10^{19} \text{ cm}^{-2}$ , as has been observed around young powerful sources at high redshift via resonant HI absorption within the Lyman- $\alpha$  emission line (Jarvis et al., 2003; Wilman et al., 2004). Redshifts of radio sources with lower HI column densities and/or higher spin temperatures could also be measured if their intrinsic linewidths were narrower, or if their continuum sources were brighter (see also Kanekar & Briggs, this volume). With HI emission detectable at low redshift, and the hope that HI absorption is close to ubiquitous at high redshift, an almost complete census of the evolution of powerful radio AGN activity may well be obtained using just the SKA.

## 7. Conclusions

In this paper we concentrate on  $z < 6$  AGN (for a discussion of higher-redshift AGN, see Carilli et al., this volume). Although detecting radio emission from  $z < 6$  AGN will be a trivial exercise for the SKA, measuring their redshifts and probing them in detail requires low-frequency capabilities. A SKA which can operate between 200 MHz  $\rightarrow$  1400 MHz would therefore be ideal for investigating AGN activity after the epoch of reionization. Here we highlight some of the science that the SKA could deliver regarding this population. We should be able to achieve the following.

- Detect all the  $> 10^6 M_{\odot}$  black holes in the observable Universe with accretion luminosities above  $\sim 0.1 L_{\text{Edd}}$ .
- Trace accretion luminosities from  $L/L_{\text{Edd}} = 1 \rightarrow 10^{-4}$  as a function of redshift up to  $z = 6$  for all black holes with  $M > 10^9 M_{\odot}$ . The SKA will also be able to probe the  $M > 10^8 M_{\odot}$  dormant ( $L/L_{\text{Edd}} < 10^{-3}$ ) black hole population out to  $z \sim 6$ .
- Constrain the evolution in the radio luminosity function for both radio-quiet and

<sup>10</sup>Assuming  $FOV = 1 \text{ deg}^2$ . If  $FOV$  was (say) 10-times higher, these features would be detected at  $\approx 30\sigma$  and weaker (lower  $N_{\text{H}}$  and higher  $T_{\text{S}}$ ) features could be detected.

<sup>11</sup>To obtain full sky coverage for HI at all redshifts in the range  $0 < z < 6$  the continuum survey will need to adopt the ‘tiling’ approach discussed in Sec. 2 of Rawlings et al. (this volume).

radio-loud AGN, up to  $z \sim 2$ , *without the need for optical follow-up time*. This is possible because the SKA will be able to detect HI emission from all massive galaxies up to this redshift for a survey in which the effective exposure time is  $\sim 4 - 20$  hours (see Rawlings et al., this volume). Constraining the luminosity function at higher redshifts, i.e. within the ‘quasar epoch’ at  $z \sim 2 \rightarrow 6$ , requires (if additional optical or near-infrared observations are to be avoided) HI absorption experiments with an SKA that operates down to 200 MHz (see also Kanekar & Briggs, this volume).

- Constrain the three-dimensional clustering of these sources, with respect to the general galaxy population (see van der Hulst et al., this volume), again without the need for optical follow-up time. This may be crucial to our understanding of how AGN activity is triggered with respect to the large-scale environment, i.e. where does the star formation occur in a cluster and where does the AGN activity occur. Does it occur along dark-matter filaments with AGN at their centres? Progress will have been made on this issue by the time the SKA starts to operate, but only the SKA will trace this evolution in an ‘all hemisphere’ sample up to  $z \sim 2$ .
- The huge cosmic volumes (in comparison to present and future optical and X-ray telescopes) surveyed by the SKA would allow investigations of the largest structures in the Universe. Brand et al. (2003) have shown that moderately powerful radio galaxies are able to trace structures on  $\sim 100$ -Mpc scales. On discovering such structures the SKA will be able to probe where the AGN and star-formation activity occurs with respect to the large-scale structure. Counts of these structures have cosmological implications (Blake et al., this volume; Rawlings et al., this volume).
- The sensitivity of the SKA to the HI line will allow extremely detailed investigations of the neutral gas surrounding the central engine, especially with VLBI capability (Morganti et al., this volume). This high column density gas ( $N_{\text{H}} > 10^{26} \text{ m}^{-2}$ ), may be responsible for the archetypal type-II quasars and could easily be detected with the SKA for any source with a moderately bright core, up to the highest redshifts. Not only will the SKA be able to detect it but it will also be able to trace the dynamics (Beswick et al., 2004). This sort of study will never be achieved with optical telescopes because the high-column densities involved lead to a heavily saturated absorption profile in Lyman- $\alpha$ .
- Measure inflows/outflows of HI gas, both in emission and absorption up to  $z \sim 2$ . The SKA would also have the power to see gas stripping by/around an AGN by tracing the HI-emitting (e.g. Kenney, van Gorkum & Vollmer, 2004). If powerful AGN lie at the interface of merging sub-clusters (e.g. Simpson & Rawlings, 2002), then the gas stripping around galaxies due to their interaction with the intra-cluster medium should be easily detectable with the SKA. Outflows of gas, driven by the AGN, may strip gas from not only the host galaxy but also neighbouring galaxies. This is one area where a multi-wavelength approach, particularly with optical/near-infrared telescopes, would enable the investigation of gas stripping along with chemical enrichment within the intracluster medium, and how this is affected by the geometry of any sub-cluster merger.
- An ‘all-hemisphere’ survey, deep enough to detect all the AGN in the Universe, and measure redshifts for all of the most powerful ones, will also provide the perfect sample for probing the magnetic fields along the line of sight via Faraday Rotation measurements (Gaensler, Beck & Feretti, this volume). As the SKA will detect AGN at all redshifts then any evolution in the magnetic fields could also be investigated with such a survey.

- The SKA would greatly benefit investigations of feedback mechanisms in the high-redshift Universe where AGN-driven feedback events may be a crucial factor in the evolution of all galaxies. In Rawlings & Jarvis (2004) we show that powerful radio jets may have a profound influence on the evolution of all galaxies surrounding the AGN. This is because the radio source is able to inject enough energy into its surroundings that it gravitationally unbinds ionized gas associated not only with its host galaxy, but more widely throughout the protoclusters in which they seem to reside (Venemans et al., 2002). This process would yield a reservoir of gas within the protocluster which is gravitationally unbound, and has been heated such that it cannot accrete back onto the protogalaxies. Hence, there will be a protocluster-wide shut down of activity, whether it be circumnuclear star formation or black-hole accretion. With the SKA we will be able to trace the neutral HI gas in such protoclusters and trace the effect that the powerful radio jets have on the protocluster environment. This will essentially be monitoring AGN feedback mechanisms *in action*, as the SKA will have both the sensitivity and the field-of-view to do this for *all* powerful AGN at *all* redshifts.

## ACKNOWLEDGEMENTS

MJJ acknowledges the support of a PPARC PDRA. SR is grateful to the UK PPARC for a Senior Research Fellowship, and for financial support from the Australia Telescope National Facility. We would also like to thank Richard Wilman for providing a suite of X-ray spectra of AGN and Nick Seymour for providing a compilation of radio source counts.

## References

- Abdalla, F. B., & Rawlings S., 2004, MNRAS, in press
- Alexander, D. M., et al. 2003a, AJ, 125, 383
- Alexander, D. M., et al. 2003b, AJ, 126, 539
- Barger, A. J., Cowie, L. L., Capak, P., Alexander, D. M., Bauer, F. E., Brandt, W. N., Garmire, G. P., & Hornschemeier, A. E. 2003a, ApJL, 584, L61
- Barger, A. J., et al. 2003b, AJ, 126, 632
- Becker, R. H., et al. 2001, AJ, 122, 2850
- Beswick, R. J., Peck, A. B., Taylor, G. B., Giovannini, G., 2004, MNRAS, in press
- Blundell, K. M., Rawlings, S., Eales, S. A., Taylor, G. B., & Bradley, A. D. 1998, MNRAS, 295, 265
- Blundell, K. M., & Rawlings, S., 2001, ApJ, 562, 5
- Brand, K., Rawlings, S., Hill, G. J., Lacy, M., Mitchell, E., Tufts, J., 2003, MNRAS, 344, 283
- Brandt, W. N., et al. 2001, AJ, 122, 2810
- Brinkmann, W., Laurent-Muehleisen, S. A., Voges, W., Siebert, J., Becker, R. H., Brotherton, M. S., White, R. L., & Gregg, M. D. 2000, A&A, 356, 445
- Chambers, K. C., Miley, G. K., van Breugel, W. J. M., & Huang, J.-S. 1996, ApJS, 106, 215
- Chengalur, J. N., & Kanekar, N., 2000, MNRAS, 318, 303
- Clewley, L. & Jarvis M. J., 2004, MNRAS, 352, 909
- Cohen, A. S., Röttgering, H. J. A., Jarvis, M. J., Kassim, N. E., Lazio T. J. W., 2004, ApJS, 150, 417
- De Breuck, C., et al. 2001, AJ, 121, 1241
- Dunlop, J. S. & Peacock, J. A. 1990, MNRAS, 247, 19
- Dunlop, J.S., McLure, R.J., Kukula, M.J., Baum, S.A., O’Dea, C.P., Hughes, D.H., 2003, MNRAS, 340,1095

- Eales, S., Rawlings, S., Law-Green, D., Cotter, G., & Lacy, M. 1997, MNRAS, 291, 593
- Elvis, M., Risaliti, G., Zamorani, G., 2002, ApJ, 565, 75
- Elvis, M., et al., 1994, ApJS, 95, 1
- Fan, X., et al. 2001, AJ, 121, 54
- Fan, X., et al. 2001, AJ, 122, 2833
- Fan, X., et al. 2003, AJ, 125, 1649
- Fanaroff, B. L. & Riley, J. M. 1974, MNRAS, 167, 31P
- Gandhi, P., Crawford, C. S., Fabian, A. C., & Johnstone, R. M. 2004, MNRAS, 348, 529
- Goldschmidt, P., Kukula, M. J., Miller, L., & Dunlop, J. S. 1999, ApJ, 511, 612
- Greve, T. R., Ivison, R. J., & Papadopoulos, P. P., 2004, A&A, 419, 99
- Grimes, J. A., Rawlings, S., & Willott, C. J. 2004, MNRAS, 349, 503
- Gunn, J. E. & Peterson, B. A. 1965, ApJ, 142, 1633
- Hine, R.G., Longair, M.S., 1979, MNRAS, 188, 111
- Hook, I. M., McMahon, R. G., Shaver, P. A., & Snellen, I. A. G. 2002, A&A, 391, 509
- Jackson, C. A. & Wall, J. V. 1999, MNRAS, 304, 160
- Jarvis, M. J. , Cruz, M. J., Cohen, A. S., Röttgering, H. J. A., Kassim, N.E., 2004, MNRAS, in press, astro-ph/0408082
- Jarvis, M. J. & Rawlings, S. 2000, MNRAS, 319, 121
- Jarvis, M. J., et al. 2001a, MNRAS, 326, 1563
- Jarvis, M. J., Rawlings, S., Eales, S., Blundell, K. M., Bunker, A. J., Croft, S., McLure, R. J., & Willott, C. J. 2001b, MNRAS, 326, 1585
- Jarvis, M. J., Rawlings, S., Willott, C. J., Blundell, K. M., Eales, S., & Lacy, M. 2001c, MNRAS, 327, 907
- Jarvis, M. J., & McLure, R. J., 2002, MNRAS, 336, L38
- Jarvis, M. J., Wilman, R. J., Röttgering, H. J. A., & Binette, L. 2003, MNRAS, 338, 263
- Kukula, M. J., Dunlop, J. S., Hughes, D. H., & Rawlings, S. 1998, MNRAS, 297, 366
- Laing, R. A., Riley, J. M., & Longair, M. S. 1983, MNRAS, 204, 151
- Lawrence, A. 1991, MNRAS, 252, 586
- Kenney, J. D. P., van Gorkom, J. H, & Vollmer, B., 2004, AJ, 127, 3361
- McLure, R. J., Jarvis, M. J., 2004, MNRAS, in press, astro-ph/0408203
- McLure, R. J., Willott, C. J., Jarvis, M. J., Rawlings S., Hill, G. J., Mitchell, E., Dunlop, J. S., Wold, M., 2004, MNRAS, 351, 347
- Miyaji, T., Hasinger, G., & Schmidt, M. 2000, A&A, 353, 25
- Norman, C., et al. 2002, ApJ, 571, 218
- Papadopoulos, P. P., Ivison, R., Carilli, C., Lewis, G., 2001, Nature, 409, 58
- Prouton, O. R., Bressan, A., Clemens, M., Franceschini, A., Granato, G. L., Silva, L., 2004, A&A, 421, 115
- Rawlings, S., Eales, S., & Lacy, M. 2001, MNRAS, 322, 523
- Rawlings, S., Jarvis, M. J., 2004, MNRAS, in press
- Rawlings, S., Lacy, M., Blundell, K. M., Eales, S. A., Bunker, A. J., & Garrington, S. T. 1996, Nature, 383, 502
- Rengelink, R. B., Tang, Y., de Bruyn, A. G., Miley, G. K., Bremer, M. N., Röttgering, H. J. A., & Bremer, M. A. R. 1997, A&AS, 124, 259

- Röttgering, H. J. A., Lacy, M., Miley, G. K., Chambers, K. C., & Saunders, R. 1994, *A&AS*, 108, 7
- Röttgering, H. J. A., van Ojik, R., Miley, G. K., Chambers, K. C., van Breugel, W. J. M., & de Koff, S. 1997, *A&A*, 326, 505
- Schneider, D. P., et al. 2003, *AJ*, 126, 2579
- Seymour, N., McHardy, I. M., & Gunn, K. F., 2004, *MNRAS*, in press (astro-ph/0404141)
- Shaver, P. A., Wall, J. V., Kellermann, K. I., Jackson, C. A., & Hawkins, M. R. S. 1996, *Nature*, 384, 439
- Simpson, C. 1998, *MNRAS*, 297, L39
- Simpson, C., & Rawlings, S., 2002, *MNRAS*, 334, 511
- Snellen, I. A. G. & Best, P. N. 2001, *MNRAS*, 328, 897
- Sopp, H., & Alexander, P., 1992, *MNRAS*, 259, 425
- Steffen, A. T., Barger, A. J., Cowie, L. L., Mushotzky, R. F., Yang, Y., 2003, *ApJ*, 596, 23
- Ueda, Y., Akiyama, M., Ohta, K., & Miyaji, T. 2003, *ApJ*, 598, 886
- van Breugel, W., De Breuck, C., Stanford, S. A., Stern, D., Röttgering, H., & Miley, G. 1999, *ApJL*, 518, L61
- van Ojik, R., Röttgering, H. J. A., Miley, G. K., & Hunstead, R. W. 1997, *A&A*, 317, 358
- Venemans, B. P., et al., 2002, *ApJ*, 569, 11
- Voges, W., et al. 1999, *A&A*, 349, 389
- Waddington, I., Dunlop, J. S., Peacock, J. A., & Windhorst, R. A. 2001, *MNRAS*, 328, 882
- Waddington, I., Windhorst, R. A., Dunlop, J. S., Koo, D. C., & Peacock, J. A. 2000, *MNRAS*, 317, 801
- White, R. L., Becker, R. H., Helfand, D. J., & Gregg, M. D. 1997, *ApJ*, 475, 479
- Wilman, R. J., Fabian, A. C., 1999, *MNRAS*, 309, 862
- Wilman, R. J., Fabian, A. C., & Nulsen, P. E. J. 2000, *MNRAS*, 319, 583
- Wilman, R. J., Jarvis, M. J., Röttgering, H. J. A., & Binette, L. 2004, *MNRAS*, 9
- Willott, C. J., Rawlings, S., Blundell, K. M., & Lacy, M. 1999, *MNRAS*, 309, 1017
- Willott, C. J., Rawlings, S., Blundell, K. M., & Lacy, M. 2000, *MNRAS*, 316, 449
- Willott, C. J., Rawlings, S., Blundell, K. M., Lacy, M., & Eales, S. A. 2001, *MNRAS*, 322, 536
- Willott, C. J., Rawlings, S., Blundell, K. M., Lacy, M., Hill, G. J., & Scott, S. E. 2002, *MNRAS*, 335, 1120
- Willott, C. J., Rawlings, S., Jarvis, M. J., & Blundell, K. M. 2003, *MNRAS*, 339, 173
- Willott, C. J., McLure, R. J., & Jarvis, M. J., 2003, *ApJ*, 587, 15